Journal of Visualized Experiments

Studying Left Ventricular Reverse Remodeling by Aortic Debanding in Rodents

--Manuscript Draft--

Article Type:	Methods Article - JoVE Produced Video
Manuscript Number:	JoVE60036R2
Full Title:	Studying Left Ventricular Reverse Remodeling by Aortic Debanding in Rodents
Keywords:	Aortic debanding, Left ventricular reverse remodeling, aortic banding, hypertrophy, pressure overload, cardiac recovery, animal model, cardiovascular diseases
Corresponding Author:	Daniela Miranda-Silva Universidade Do Porto Porto, Porto PORTUGAL
Corresponding Author's Institution:	Universidade Do Porto
Corresponding Author E-Mail:	daniela.miranda143@gmail.com
Order of Authors:	Daniela Miranda-Silva
	Patricia Goncalves-Rodrigues
	Adelino F Leite-Moreira
	Inês Falcão-Pires
Additional Information:	
Question	**Response**
Please indicate whether this article will be Standard Access or Open Access.	Standard Access (US$2,400)
Please indicate the **city, state/province, and country** where this article will be **filmed**. Please do not use abbreviations.	Porto, Portugal

TITLE:

Studying Left Ventricular Reverse Remodeling by Aortic Debanding in Rodents

AUTHORS AND AFFILIATIONS:

Patrícia Goncalves-Rodrigues[1]*, Daniela Miranda-Silva[1]*, Adelino F Leite-Moreira[1], Inês Falcão-Pires[1]

[1]Unidade de Investigação Cardiovascular, Departamento de Cirurgia e Fisiologia, Faculdade de Medicina, Universidade do Porto, Portugal.

*These authors contributed equally

Corresponding author:

Inês Falcão Pires (ipires@med.up.pt)

Email Addresses of Co-authors:

Patrícia Rodrigues (rodrigues13patricia@gmail.com)

Daniela Miranda-Silva (daniela.miranda143@gmail.com)

Adelino F. Leite-Moreira (amoreira@med.up.pt)

KEYWORDS:

Aortic debanding, Left ventricular reverse remodeling, aortic banding, hypertrophy, pressure overload, cardiac recovery, animal model, cardiovascular diseases

SUMMARY:

Here we describe a step-by-step protocol of surgical aorta debanding in the well-established mice model of aortic-constriction. This procedure not only allows studying the mechanisms underlying the left ventricular reverse remodeling and regression of hypertrophy but also to test novel therapeutic options that might accelerate myocardial recovery.

LONG ABSTRACT:

To better understand the left ventricular (LV) reverse remodeling (RR), we describe a rodent model wherein, after aortic banding-induced LV remodeling, mice undergo RR upon removal of the aortic constriction. In this paper, we describe a step-by-step procedure to perform a minimally invasive surgical aortic debanding in mice. Echocardiography was subsequently used to assess the degree of cardiac hypertrophy and dysfunction during LV remodeling and RR and to determine the best timing for aortic debanding. At the end of the protocol, terminal hemodynamic evaluation of the cardiac function was conducted, and samples were collected for histological studies. We showed that debanding is associated with surgical survival rates of 70-80%. Moreover, two weeks after debanding, the significant reduction of ventricular afterload triggers the regression of ventricular hypertrophy (~20%) and fibrosis (~26%), recovery of diastolic dysfunction as assessed by the normalization of left ventricular filling and end-diastolic pressures (E/e' and LVEDP). Aortic debanding is a useful experimental model to study LV RR in rodents. The extent of myocardial recovery is variable between subjects, therefore, mimicking

the diversity of RR that occurs in the clinical context, such as aortic valve replacement. We conclude that the aortic banding/debanding model represents a valuable tool to unravel novel insights into the mechanisms of RR, namely the regression of cardiac hypertrophy and the recovery of diastolic dysfunction.

INTRODUCTION:

The constriction of the transverse or ascending aorta in the mouse is a widely used experimental model for pressure overload-induced cardiac hypertrophy, diastolic and systolic dysfunction and heart failure[1-4]. Aortic-constriction initially leads to compensated left ventricle (LV) concentric hypertrophy to normalize wall stress[1]. However, under certain circumstances, such as prolonged cardiac overload, this hypertrophy is insufficient to decrease the wall stress, triggering diastolic and systolic dysfunction (pathological hypertrophy)[5]. In parallel, changes in extracellular matrix (ECM) lead to the collagen deposition and crosslinking in a process known as fibrosis, which can be subdivided into replacement fibrosis and reactive fibrosis. Fibrosis is, in most of the cases, irreversible and compromises myocardial recovery after overload relief[6,7]. Nevertheless, recent cardiac magnetic resonance imaging studies revealed that reactive fibrosis is able to regress in the long term[8]. Altogether, fibrosis, hypertrophy and cardiac dysfunction are the part of a process known as myocardial remodeling that rapidly progresses towards heart failure (HF).

Understanding the features of myocardial remodeling has become a major objective for limiting or reversing its progression, the latter known as reverse remodeling (RR). The term RR includes any myocardial alteration chronically reversed by a given intervention, such pharmacological therapy (e.g., antihypertensive medication), valve surgery (e.g., aortic stenosis) or ventricular assist devices (e.g., chronic HF). However, RR is often incomplete due to the prevailing hypertrophy or systolic/diastolic dysfunction. Thus, the clarification of RR underlying mechanisms and novel therapeutic strategies are still missing, which is mostly due to the impossibility to access and study human myocardial tissue during RR in most of these patients.

To overcome this limitation, rodent models have played a significant role in advancing our understanding of the signaling pathways involved in HF progression. Specifically, aortic debanding of mice with an aortic constriction represents a useful model to study the molecular mechanisms underlying adverse LV remodeling[9] and RR[10,11] as it allows the collection myocardial samples at different time points in these two phases. Moreover, it provides an excellent experimental setting to test potential novel targets that can promote/accelerate RR. For instance, in aortic stenosis context, this model might provide information about the molecular mechanisms involved in the vast diversity of myocardial response underlying the (in)completeness of the RR[6,12], as well as, the optimal timing for valve replacement, which represents a major shortcoming of the current knowledge. Indeed, the optimal timing for this intervention is a subject of debate, mainly because it is defined based on the magnitude of aortic gradients. Several studies advocate that this time point might be too late for the myocardial recovery as fibrosis and diastolic dysfunction are often already present[12].

To our knowledge, this is the only animal model that recapitulates the process of both myocardial remodeling and RR taking place in conditions such as aortic stenosis or hypertension before and

after valve replacement or the onset of anti-hypertensive medication, respectively.

Seeking to address the challenges summarized above, we describe a surgical animal model that can be implemented both in mice and rats, addressing the differences between these two species. We describe the main steps and details involved when carrying out these surgeries. Finally, we report the most significant changes taking place in the LV immediately before and throughout RR.

PROTOCOL:

All animal experiments comply with the Guide for the Care and Use of Laboratory Animals (NIH Publication no. 85–23, revised 2011) and the Portuguese law on animal welfare (DL 129/92, DL 197/96; P 1131/97). The competent local authorities approved this experimental protocol (018833). Seven-week-old male C57B1/J6 mice were maintained in appropriate cages, with a regular 12/12 h light-dark cycle environment, a temperature of 22 °C and 60% humidity with access to water and a standard diet ad libitum.

1. Preparation of the surgical field

1.1. Disinfect the operation site with 70% alcohol and place a disposable operating room table cover over the surgical area.

1.2. Sterilize all the instruments before surgery.

NOTE: This procedure requires micro surgical scissors, 2 fine curved forceps, 3 fine straight, a scalpel, small forceps, an angled dissector scissor, a needle holder, an ultrafine ligation aid, 2 hemostats and, lastly, a magnetic fixator retraction system is highly recommended (**Figure 1A**).

1.3. Curve the tip of a 26 G blunted needle to 90° for an easier approach to the aorta. A 26 G needle will create a 0.45 mm diameter aortic narrowing (**Figure 1B**).

1.4. Adjust the heating pad temperature to 37 ± 0.1 °C.

2. Mice preparation and intubation

2.1. Anesthetize young C57B1/J6 mice (20-25 g) by inhalation of 8% sevoflurane with 0.5 - 1.0 L/min 100% O_2 in a cone tube.

2.2. Check the anesthesia depth using the toe pinch withdrawal reflex.

2.3. Place the mouse at dorsal recumbency on an inclined plate and proceed to orotracheal intubation.

2.4. Move the mouse to the heating pad and quickly connect the orotracheal tube to the ventilator to initiate the mechanical ventilation.

2.5. Adjust the ventilator parameters to a frequency of 160 breaths/min and a tidal volume of 10 mL/Kg.

3. Preparation for surgery (for both banding and debanding surgeries)

3.1. Shave and apply the depilatory cream from the neckline to mid-chest level of the mice.

3.2. Apply ophthalmic gel to the animals' eyes to prevent drying out of the cornea.

3.3. Place a rectal probe and the oximeter at the paw or tail for monitoring temperature, blood oxygenation, and heart rate, respectively.

NOTE: Anesthesia induces significant hypothermia, therefore, it is important to maintain normal body temperature during surgery to avoid a rapid decrease in heart rate.

3.4. Maintain anesthesia with sevoflurane (2.0 - 3.0%). Check the correct level of anesthesia by the lack of the toe-pinch reflex.

3.5. Place the mice in right-lateral decubitus on a heating pad and secure the limbs to the magnetic fixator retraction system with a tape to keep the animal in the correct position during the surgery (**Figure 2, Figure 3A**).

3.6. Disinfect the mouse chest with 70% alcohol followed by providone-iodine solution.

4. Ascending aortic banding surgery

NOTE: For a detailed protocol description, consult [2-4,13].

4.1. With a disposable blade, perform a small (~0.5 cm) skin incision on the left side immediately below the axilla level and dissect the skin.

4.2. Gently dissect and separate the pectoralis muscle and other muscle layers until the ribs become visible. Use fine forceps and avoid cutting the muscle.

4.3. Under a microscope, identify the intercostal spaces and open a small incision between the 2nd and 3rd intercostal space with fine forceps.

4.4. Retract the ribs by placing the chest retractor (**Figure 2A**).

4.5. Use small forceps to gently dissect and separate the thymic lobes until ascending aorta becomes visible.

NOTE: Cotton applicators should be handy in case of bleeding. Warm sterile saline should be

given subcutaneously in case of significant bleeding (e.g., the mammary artery).

4.6. Use small forceps to gently dissect the aorta.

NOTE: Aorta is considered to be dissected when there are no fat or other adhesions around it and it is possible to easily encircle the vessel with a small curve forceps.

4.7. After aortic dissection, place a 7-0 polypropylene ligature around aorta by using ligation aid and curved forceps (**Figure 2B)**.

4.8. Position the blunted 26 G needle parallel to the aorta (tip pointed towards the mice head) (**Figure 2B)**. For mice weighing 20-25 g, this needle induces a reproducible 65-70% aortic constriction.

4.9. Make 2 loose knots around the aorta and the 26 G needle with the help of 2 forceps (**Figure 2B)**.

4.10. Tighten the 1st knot and, quickly after, the 2nd knot. Briefly confirm the right positioning of the constriction and quickly remove the needle to restore aortic blood flow. Finally, make a 3rd knot (BA group).

4.11. Reposition the thymus and the muscles into their initial position.

4.12. Perform the sham procedure identical to the constriction procedure but keeping the suture loose around the aorta (SHAM group).

4.13. Cut the ends of the suture and remove the chest retractor.

NOTE: Short suture ends may increase the probability of knots loosening with aortic pressure, while long ends make the debanding procedure riskier since adhesions can occur between the suture and the left atrium.

4.14. Close the chest wall using 6-0 polypropylene suture with a simple interrupted or continuous suture using the lowest number of stitches possible. Tighten the last chest knot with the lungs inflated at end inspiration by pinched off the outflow of the ventilator for 2s to re-inflate the lungs.

4.15. Close the skin with a 6-0 silk/polypropylene suture in a continuous suture pattern.

NOTES: If a more recent ventilator is used, it is possible to programme it to pause in inspiration (Setup-Advanced-Pause-Inspiration)

5. Post-operative care

5.1. Apply providone-iodine solution to the skin suture site.

5.2. For proper analgesia, administer buprenorphine subcutaneously 0.1 mg/Kg, twice daily, until the animal fully recovers (usually 2-3 days after surgery).

5.3. Inject sterile saline intraperitoneally to prevent dehydration in case of significant bleeding during the surgery.

5.4. Turn off the anesthesia (without deintubating the mouse) and wait until the animal recover the reflexes (whiskers movements are an awakening signal) and starts to breathe spontaneously.

5.5. Remove the tracheal cannula.

5.6. Let the animal recover in an incubator at 33 °C.

5.7. Return the animal to a 12 h light/dark cycle room after full recovery.

6. Aortic debanding surgery

6.1. Seven weeks later, perform the debanding of the aorta in half of the BA animals and remove the loose suture from half of the SHAM mice, giving rise to 2 new groups – debanding (DEB) and DE(SHAM), respectively. DE(SHAM) represents the control for the DEB group (**Figure 4**).

6.2. Repeat all the steps 2.1 to 3.6 mentioned above.

6.3. Gently dissect the tissues, adhesions, and fibrosis around the aorta until its constriction becomes visible.

6.4. Carefully dissect the aorta and separate the suture from the aorta. Cut the suture with angled one-probed spring scissors (**Figure 3B**).

6.5. Close the chest wall using 6-0 polypropylene suture with a simple interrupted or continuous suture using the minimum number of stitches possible.

NOTE: Try to tighten the last chest suture when lungs are inflated to avoid pneumothorax.

6.6. Close the skin with a 6-0 silk/polypropylene suture in a continuous suture pattern.

6.7. Perform all post-operative care procedures as mentioned in 5.

6.8. Sacrifice the animals 2 weeks later.

7. Echocardiography to assess cardiac function and left ventricular hypertrophy in vivo

7.1. Perform the echocardiographic exam every 2-3 weeks to follow the progression of hypertrophy and cardiac function.

7.2. Anesthetize the animals, as described, by inhalation of 5% sevoflurane with a nose cone. Adjust the anesthesia level by decreasing it to 2.5%.

7.3. Shave and apply the depilatory cream from the neckline to mid-chest level.

7.4. Place the animal on a heating pad and place the ECG electrodes. Assure a good ECG trace and maintain heart rate between 300 and 350 beats/min.

7.5. Monitor the temperature (~37 °C).

7.6. Apply echo gel and position the animal at left lateral decubitus.

7.7. Start the echocardiograph and adjust the settings.

7.8. Position an ultrasound probe over the thorax.

7.9. Assess the pressure gradient across the banding at 7 and 2 weeks after banding and debanding surgery, respectively. Position the probe at the LV long axis and place the beam over aorta. Press the button PW to activate pulsed wave Doppler echocardiography. After seven weeks of banding, aortic gradients will be >25 mmHg in the banded animals.

7.10. Record two-dimensional guided images of aorta showing the presence or absence of the ascending aorta constriction to anatomically visualize the efficacy of the banding and debanding.

NOTE: It is possible to visualize turbulent flow at the constriction level if the color mode is available.

7.11. Assess hypertrophy by positioning the probe at an LV short axis, at papillary muscles level, and press M-mode tracing to visualize LV anterior wall (LVAW), LV diameter (LVD) and LV posterior wall (LVPW) in diastole (D) and systole (S) (**Figure 5**).

7.12. Assess systolic function, calculate the ejection fraction and fractional shortening as previously described[14,15].

7.13. Assess diastolic function by 1) determining the peak of pulsed-wave Doppler of early and late mitral flow velocity (E and A waves, respectively) using an apical 4-chamber apical view just above the mitral leaflets; 2) recording lateral mitral annular myocardial early diastolic (E') and peak systolic (S') velocities using pulsed-TDI and apical 4-chamber apical view (**Figure 5**).

7.14. Record at least three consecutive heartbeats to each parameter assessment. These values will be subsequently averaged.

8. Hemodynamic assessment

8.1. At the end of the protocol (**Figure 4**), perform final echocardiography, as described in 7, before the terminal hemodynamic assessment.

8.2. Repeat steps 2.1 to 3.6.

8.3. Cannulate the right jugular vein and perfuse sterile saline at 64 mL/Kg/h.

8.4. Rotate slightly the animal to the left side and make a skin incision at the level of the xiphoid appendix.

8.5. Separate the skin from the muscle with forceps or with a scissor.

8.6. Make a lateral incision between the left ribs at the xiphoid appendix level.

8.7. Perform a left lateral thoracotomy to expose the heart fully.

NOTE: To avoid bleeding and lung damage, insert a cotton swab into the thoracic cavity and push the lung gently while inserting two hemostats on the right and left side of the place to cut.

8.8. Pre-heat the P-V loop catheters in a water-bath at 37 °C.

8.9. Calibrate the catheter (setup, channel setting, chose the correct channel for pressure and volume, units).

8.10. Insert a catheter apically into the LV and assure the volume sensors are positioned between the aortic valve and the apex. Volumes can be assessed by echocardiography (**Figure 5)**. Visualization of the pressure-volume loops helps to confirm the correct positioning of the catheter (**Figure 6).**

8.11. Allow the animal to stabilize 20-30 min without significant changes in the shape of the pressure-volume loops.

8.12. With ventilation suspended at end-expiration, acquire baseline recordings(**Figure 6)**. Continuously acquire data at 1,000 Hz to be subsequently analyzed off-line by appropriate software.

8.13. Compute parallel conductance after the hypertonic saline bolus (10%, 10 µL).

8.14. While anesthetized, sacrifice the animal by exsanguination, collect and centrifuge the blood.

8.15. Lastly, excise and collected the heart. Weight the heart, the left, and the right ventricle separately and immediately store the samples in liquid nitrogen or formalin for subsequent molecular or histological studies, respectively.

9. Aortic banding/debanding procedure in rats

9.1. Perform aortic banding in young Wistar (70-90 g) using a 22 G needle and 6-0 polypropylene ligature to constrict the aorta.

9.2. Ensure a proper anesthetic and analgesic procedures with 3-4% of sevoflurane and 0.05 mg/Kg of buprenorphine for, respectively.

9.3. During echocardiography, assure a heart rate always above 300 rate / min (ideally between 300 and 350).

9.4. Before step 8.9, gently dissect the rat aorta, place a flow probe around it to measure cardiac output. The use of the aortic flow probe is the gold standard procedure for rats.

9.5. For the hemodynamic evaluation, cannulate the jugular or femoral vein for fluid administration (32 mL/Kg/h).

9.6. Replace the pressure-volume catheter SPR-1035 by the SPR-847 or SPR-838, whose sizes better suit the rat ventricular dimensions.

REPRESENTATIVE RESULTS:

Post-operative and late survival

The perioperative survival of the banding procedure is 80% and the mortality during the first month is typically <20%. As previously mentioned, the success of the debanding surgery is highly dependent on how invasive the previous surgery was. After a learning curve, the mortality rate during the debanding procedures is around 25%. For this mortality accounts mostly deaths during the surgery procedure, including aorta or left atrium rupture (in rats, the survival rate is higher in both surgical procedures).

Aortic banding and myocardial remodeling

The success of aortic constriction was verified by increased LV end-systolic pressure (LVESP) and by Doppler aortic flow velocities >2.5 m/s, which corresponds to a pressure gradient of 25 mmHg using the modified Bernoulli equation (**Figure 5**). Compared to SHAM mice, banding induced LV hypertrophy as assessed by increased LV mass (**Table 1** and **Figure 5**) and impaired diastolic function evident by higher filling pressures (ratio of mitral peak velocity of early filling (E) to early diastolic mitral annular velocity (E'), (E/e'), and left ventricular end-diastolic pressure (LVEDP) and prolonged relaxation (τ, **Table 1, Figure 5,** and **Figure 6**) within 7 weeks. Ejection fraction was still preserved at this stage of the disease.

Histologically, seven-weeks of aortic banding induced significant cardiomyocyte hypertrophy and

fibrosis (**Figure 7**).

Aortic debanding and myocardial reverse remodeling

In mice subjected to debanding, successful removal of aortic stenosis was verified by echo-Doppler velocities (**Table 1** and **Figure 5**). Debanding surgery gave rise to two groups of animals with distinct degrees of RR (DEB-COMP and DEB-INCOM), whose average values are shown in table 1. Overall, debanding promoted a significant decrease of afterload (decreased LVESP) and LV hypertrophy (assessed by morphometry, echocardiography, and histology). Moreover, we observed normalization of diastolic function and aortic velocities (**Table 1**, **Figure 5, Figure 6**, and **Figure 7**).

FIGURE AND TABLE LEGENDS:

Table 1: Left ventricle morphofunctional changes assessed by echocardiography and by hemodynamics.

Table 2: Critical steps of the protocol.

Figure 1: Ultra-fine surgical instruments used for the banding and debanding procedures. (**A**) 2 needle-holders and a scalpel blade; two catheters for mice intubation and a scissor; a scalpel, 2 curved forceps, a ligation aid, a microsurgical scissor, 3 straight forceps; (**B**) and 26G-needle and blunted 26G-needle curved to fit the mice small thoracic opening properly.

Figure 2: **Aortic banding procedure.** (**A**) The thoracic approach to the ascending aorta performed with the help of a magnetic fixator retraction system (3 retractors are visible). (**B**) The ascending aorta is clearly dissected and visible. The blunted needle and the polypropylene suture 6-0 are placed in the right position to perform the aortic banding.

Figure 3: Aortic debanding procedure. (**A**) The mouse is placed in a magnetic retraction system, representing a handy tool to retract the muscles and tissues around the aorta. The mouse is intubated for mechanical ventilation. A rectal probe controls temperature and an oximeter is placed on the right mice paw to monitor blood oxygenation during surgery. Fibrosis and adherent tissue is carefully removed around the aorta and suture, to be able to cut the suture (**B**) and (**C**).

Figure 4: Experimental protocol design for mice. Myocardial remodeling (red) and reverse remodeling (green) are shown in the bottom together with all evaluation tasks. Of note, debanding surgery can give rise to two groups of animals with distinct degrees of reverse remodeling. Thus, we obtained DEB mouse with complete (DEB-COMP) and incomplete (DEB-INCOM) myocardial recovery.

Figure 5: Echocardiographic assessment of cardiac structure and function. (**A**) Aortic flow velocities; (**B**) LV mass; (**C**) Ventricular dimensions (LV diameter, LVD) and wall thickness (LV posterior wall, LVPW and LV anterior wall, LVAW); (**D**) Transmitral flow (peak of pulse Doppler wave of late mitral flow velocity, A, and peak of pulsed Doppler wave of early mitral flow velocity,

E) and (**E**) Myocardial velocities (late diastolic mitral annular tissue velocity, A'; early diastolic mitral annular tissue velocity, E' and systolic mitral annular tissue velocity, S').

Figure 6: Representative pressure-volume loops for SHAM, BA and DEB groups. Data were continuously acquired at 1000 Hz and subsequently analyzed off-line by PVAN software.

Figure 7: Myocardial hypertrophy and fibrosis assessed histologically. (**A**) Left ventricle hypertrophy assessed by cardiomyocytes sectional area of hematoxylin-eosin (HE)-stained sections (5 µm) from SHAM (n = 17), BA (n = 14) and DEB group (n = 12). (**B**) Left Ventricular interstitial fibrosis and representative images of Red Sirius-stained sections (5 µm) from SHAM (n = 17), BA (n = 13) and DEB (n = 12).

DISCUSSION:

The model proposed herein mimics the process of LV remodeling and RR after aortic banding and debanding, respectively. Therefore, it represents an excellent experimental model to advance our knowledge on the molecular mechanisms involved in the adverse LV remodeling and to test novel therapeutic strategies able to induce myocardial recovery of these patients. This protocol details steps on how to create a rodent animal model of aortic banding and debanding with a minimally invasive and highly conservative surgical technique to reduce the surgical trauma.

The most critical step of the protocol is related to the degree of surgical aggression during aortic banding. The success of the subsequent aortic debanding surgery depends enormously on a minimally invasive banding procedure that avoids tissue aggression and fibrosis around the aorta and, therefore, a less-invasive approach is mandatory (**Table 2**). Suture internalization is associated with less LV hypertrophy and better cardiac function[16] (**Table 2**) and makes the debanding procedure impossible to perform without causing an aortic rupture. In the present study, we tried to use silk, since it creates more scar tissue at the banding site, triggering a more stable degree of pressure overload. However, in our hands, the debanding surgery was more demanding when silk was used since it is a multifilament wire making it´s total removal from the aorta more difficult. Nevertheless, these are technical issues that are widely protocol-and-operator-dependent, and these variations, type of suture, is not incompatible with good technical practices and reproductive results. Physiological parameters monitoring during banding and especially during debanding is mandatory for the success of the model implementation (**Table 2**).

In 1991, Rockman et al., described the transverse aorta constriction (TAC) in mouse for the first time[4]. Since then a considerable amount of papers came out providing numerous versions of this procedure with variations with respect to the animal age/size[17], mice genetic background[18], the diameter of the needle/constriction[19], the material used for banding, the aortic location of the banding, the duration of the banding[19] and debanding[11]. All these methodological alternatives are valid as long as they fulfill the aims of each study. However, we should stress out that the progression of the disease towards heart failure is faster and thus RR is more incomplete when selecting: 1) longer banding durations, 2) heavier/older the mice[20] and 3) smaller needle diameter used for the aortic constriction (higher percentage of aortic constriction)[16].

The duration of the banding and the debanding significantly impact the stage of the disease and, therefore, the recovery during RR. Likewise, choosing the right timing for debanding is mandatory to adjust to the severity of the disease envisaged. The results observed in our study are in accordance with pre-existence animal[11,21] and human studies[22], except for cardiomyocytes hypertrophy, where some studies showed its normalization[10,21] and others its partial regression[23]. Moreover, studies have shown that, fibrosis regression can occur in the long term (70 months for human patients)[24]. The results seem to be dependent on the technique used to address fibrosis[25]. Recently, Treibel et al. were able to differentiate between cellular (myocytes, fibroblast, endothelial, red blood cells) and extracellular (ECM, blood plasma) compartments in patients with aortic stenosis after aortic valve replacemennt (AVR) using cardiovascular magnetic resonance with T1 mapping[22]. They described that regression of LV mass following AVR can be driven by 1) matrix regression alone, where the extracellular volume reduces; 2) cellular regression alone, where extracellular volume increases; 3) or by a proportional regression in cellular and matrix compartments, where the extracellular volume is unchanged[22]. These authors concluded that, following AVR, while diffuse fibrosis and myocardial cellular hypertrophy regress, focal fibrosis does not resolve. Thus, diffuse interstitial fibrosis, as assessed by matrix volume, is a potential therapeutic target. In our study, reduction of fibrosis seems to occur within 2 weeks of RR and before cardiomyocytes hypertrophy normalization. Also, sacrificing the animals 2 weeks after the debanding was the perfect timing to obtain ventricular diversity among DEB group, namely animals with diastolic dysfunction persistence (DEB-INCOM) and others with complete LV mass reversal and diastolic function improvement (DEB-COM). Moreover, as soon as 2 weeks after debanding, we have previously shown significant right ventricular changes in the banding group that partially recover after debanding[26], while Bjornstad et al. reported normalization of fetal genes expression, indicative of myocardial remodeling within the same timeframe[11].

The surgical procedure of banding/debanding can also be performed in rats[26], however, some differences should be highlighted. Due to its bigger size, rats have more muscle layers than mice which decreases aortic visualization and hinders positioning the ligature around the aorta. On the other hand, the risk of damaging adjacent tissues and organs, such as atria or lungs, are minimized. To overcome the issue of suture internalization we used a larger polypropylene ligature in rats to hold tight the aorta (6.0 instead of 7.0 polypropylene).

Due to aorta manipulation, debanding surgery might decrease cardiac output by imposing additional afterload on LV and thus impair the circulatory and respiratory system. Compared to mice, rats seem to be more resistant to more extended anesthetic period and therefore are easier to keep the physiological respiratory parameters controlled during the long debanding surgery. In rats, LV hypertrophy development is faster than mice, but it takes longer to progress to heart failure. Thus, the debanding surgery can be done between 5-9 weeks after banding procedure without compromising ejection fraction[26].

The major limitation of the banding/debanding animal model is the demanding microsurgical skills and technique of the operator, usually requiring a long learning curve to accomplish the

debanding surgery. Another limitation is the impossibility to perform close chest hemodynamics in mouse and rat, which will be more physiologic. However, by using this method is obligatory to insert the catheter from the right carotid artery to LV which is, in this particular case not feasible since in banding animals ascending aorta is constricted before the carotid branches. Moreover, in mouse, we were not able to measure load-independent contractility (ESPVR) and diastolic parameters (slope of EDPVR) by performing vena cava occlusion maneuver, an important parameter for an adequate characterization of myocardial function. We found this maneuver difficult to perform in mice with ascending aorta constriction due to their small size (20-25g).

Future application of the banding/debanding animal model includes the development of novel therapeutic approaches to myocardial diseases and the characterization of the pathways that underlie the process of LV remodeling and RR.

In conclusion, this clinically-relevant model allows to temporally and mechanistically characterize the progression towards HF, as well as, its recovery since it allows the collection of myocardial samples in different stages of myocardial remodeling and RR. Moreover, it proves to be a useful experimental model for testing therapeutic strategies aimed at the recovery of the failing heart.

ACKNOWLEDGMENTS:

The authors thank Portuguese Foundation for Science and Technology (FCT), European Union, Quadro de Referência Estratégico Nacional (QREN), Fundo Europeu de Desenvolvimento Regional (FEDER) and Programa Operacional Factores de Competitividade (COMPETE) for funding UnIC (UID/IC/00051/2013) research unit. This project is supported by FEDER through COMPETE 2020 – Programa Operacional Competitividade E Internacionalização (POCI), the project DOCNET (NORTE-01-0145-FEDER-000003), supported by Norte Portugal regional operational programme (NORTE 2020), under the Portugal 2020 partnership agreement, through the European Regional Development Fund (ERDF), the project NETDIAMOND (POCI-01-0145-FEDER-016385), supported by European Structural And Investment Funds, Lisbon's regional operational program 2020. Daniela Miranda-Silva and Patrícia Rodrigues are funded by Fundação para a Ciência e Tecnologia (FCT) by fellowship grants (SFRH/BD/87556/2012 and SFRH/BD/96026/2013 respectively).

DISCLOSURES:

The authors have no conflict of interest.

REFERENCES:

1 Arany, Z. et al. Transverse aortic constriction leads to accelerated heart failure in mice lacking PPAR-gamma coactivator 1alpha. *Proceedings of the National Academy of Science U. S. A.* **103** (26), 10086-10091, (2006).

2 Tavakoli, R., Nemska, S., Jamshidi, P., Gassmann, M., Frossard, N. Technique of Minimally Invasive Transverse Aortic Constriction in Mice for Induction of Left Ventricular Hypertrophy. *Journal of Visualized Experiment.* 10.3791/56231 (127), (2017).

3 Zaw, A. M., Williams, C. M., Law, H. K., Chow, B. K. Minimally Invasive Transverse Aortic Constriction in Mice. *Journal of Visualized Experiment.* 10.3791/55293 (121), (2017).

4 Rockman, H. A. et al. Segregation of atrial-specific and inducible expression of an atrial natriuretic factor transgene in an in vivo murine model of cardiac hypertrophy. *Proceedings of the National Academy of Science U. S. A.* **88** (18), 8277-8281, (1991).
5 Koide, M. et al. Premorbid determinants of left ventricular dysfunction in a novel model of gradually induced pressure overload in the adult canine. *Circulation.* **95** (6), 1601-1610, (1997).
6 Rodrigues, P. G., Leite-Moreira, A. F., Falcao-Pires, I. Myocardial reverse remodeling: how far can we rewind? *American Journal of Physiology-Heart and Circulatory Physiology.* **310** (11), H1402-1422, (2016).
7 Weidemann, F. et al. Impact of myocardial fibrosis in patients with symptomatic severe aortic stenosis. *Circulation.* **120** (7), 577-584, (2009).
8 Bing, R. et al. Imaging and Impact of Myocardial Fibrosis in Aortic Stenosis. *JACC Cardiovascular Imaging.* **12** (2), 283-296, (2019).
9 Conceicao, G., Heinonen, I., Lourenco, A. P., Duncker, D. J., Falcao-Pires, I. Animal models of heart failure with preserved ejection fraction. *Netherlands Heart Journal.* **24** (4), 275-286, (2016).
10 Weinheimer, C. J. et al. Load-Dependent Changes in Left Ventricular Structure and Function in a Pathophysiologically Relevant Murine Model of Reversible Heart Failure. *Circulation Heart Failure.* **11** (5), e004351, (2018).
11 Bjornstad, J. L. et al. A mouse model of reverse cardiac remodelling following banding-debanding of the ascending aorta. *Acta Physiologica (Oxford).* **205** (1), 92-102, (2012).
12 Yarbrough, W. M., Mukherjee, R., Ikonomidis, J. S., Zile, M. R., Spinale, F. G. Myocardial remodeling with aortic stenosis and after aortic valve replacement: mechanisms and future prognostic implications. *Journal of Thoracic and Cardiovascular Surgery.* **143** (3), 656-664, (2012).
13 deAlmeida, A. C., van Oort, R. J., Wehrens, X. H. Transverse aortic constriction in mice. *Journal of Visualized Experiment.* 10.3791/1729 (38), (2010).
14 Hamdani, N. et al. Myocardial titin hypophosphorylation importantly contributes to heart failure with preserved ejection fraction in a rat metabolic risk model. *Circulation: Heart Failure.* **6** (6), 1239-1249, (2013).
15 Li, L. et al. Assessment of Cardiac Morphological and Functional Changes in Mouse Model of Transverse Aortic Constriction by Echocardiographic Imaging. *Journal of Visualized Experiment.* 10.3791/54101 (112), (2016).
16 Lygate, C. A. et al. Serial high resolution 3D-MRI after aortic banding in mice: band internalization is a source of variability in the hypertrophic response. *Basic Research in Cardiology.* **101** (1), 8-16, (2006).
17 Platt, M. J., Huber, J. S., Romanova, N., Brunt, K. R., Simpson, J. A. Pathophysiological Mapping of Experimental Heart Failure: Left and Right Ventricular Remodeling in Transverse Aortic Constriction Is Temporally, Kinetically and Structurally Distinct. *Frontiers in Physiology.* **9** 472, (2018).
18 Garcia-Menendez, L., Karamanlidis, G., Kolwicz, S., Tian, R. Substrain specific response to cardiac pressure overload in C57BL/6 mice. *American Journal of Physiology-Heart and Circulation Physiology.* **305** (3), H397-402, (2013).
19 Melleby, A. O. et al. A novel method for high precision aortic constriction that allows for generation of specific cardiac phenotypes in mice. *Cardiovascular Research.* **114** (12), 1680-1690, (2018).

20 Li, Y. H. et al. Effect of age on peripheral vascular response to transverse aortic banding in mice. *The Journal of Gerontology. Series A, Biological Sciences and Medical Sciences.* **58** (10), B895-899, (2003).
21 Ruppert, M. et al. Myocardial reverse remodeling after pressure unloading is associated with maintained cardiac mechanoenergetics in a rat model of left ventricular hypertrophy. *American Journal of Physiology-Heart and Circulation Physiology.* **311** (3), H592-603, (2016).
22 Treibel, T. A. et al. Reverse Myocardial Remodeling Following Valve Replacement in Patients With Aortic Stenosis. *Journal of the American College of Cardiology.* **71** (8), 860-871, (2018).
23 Dadson, K. et al. Cellular, structural and functional cardiac remodelling following pressure overload and unloading. *International Journal of Cardiology.* **216** 32-42, (2016).
24 Krayenbuehl, H. P. et al. Left ventricular myocardial structure in aortic valve disease before, intermediate, and late after aortic valve replacement. *Circulation.* **79** (4), 744-755, (1989).
25 McCann, G. P., Singh, A. Revisiting Reverse Remodeling After Aortic Valve Replacement for Aortic Stenosis. *Journal of the American College of Cardiology.* **71** (8), 872-874, (2018).
26 Miranda-Silva, D. et al. Characterization of biventricular alterations in myocardial (reverse) remodelling in aortic banding-induced chronic pressure overload. *Science Reports.* **9** (1), 2956, (2019).

Figure 1

Click here to access/download;Figure;Image1.png

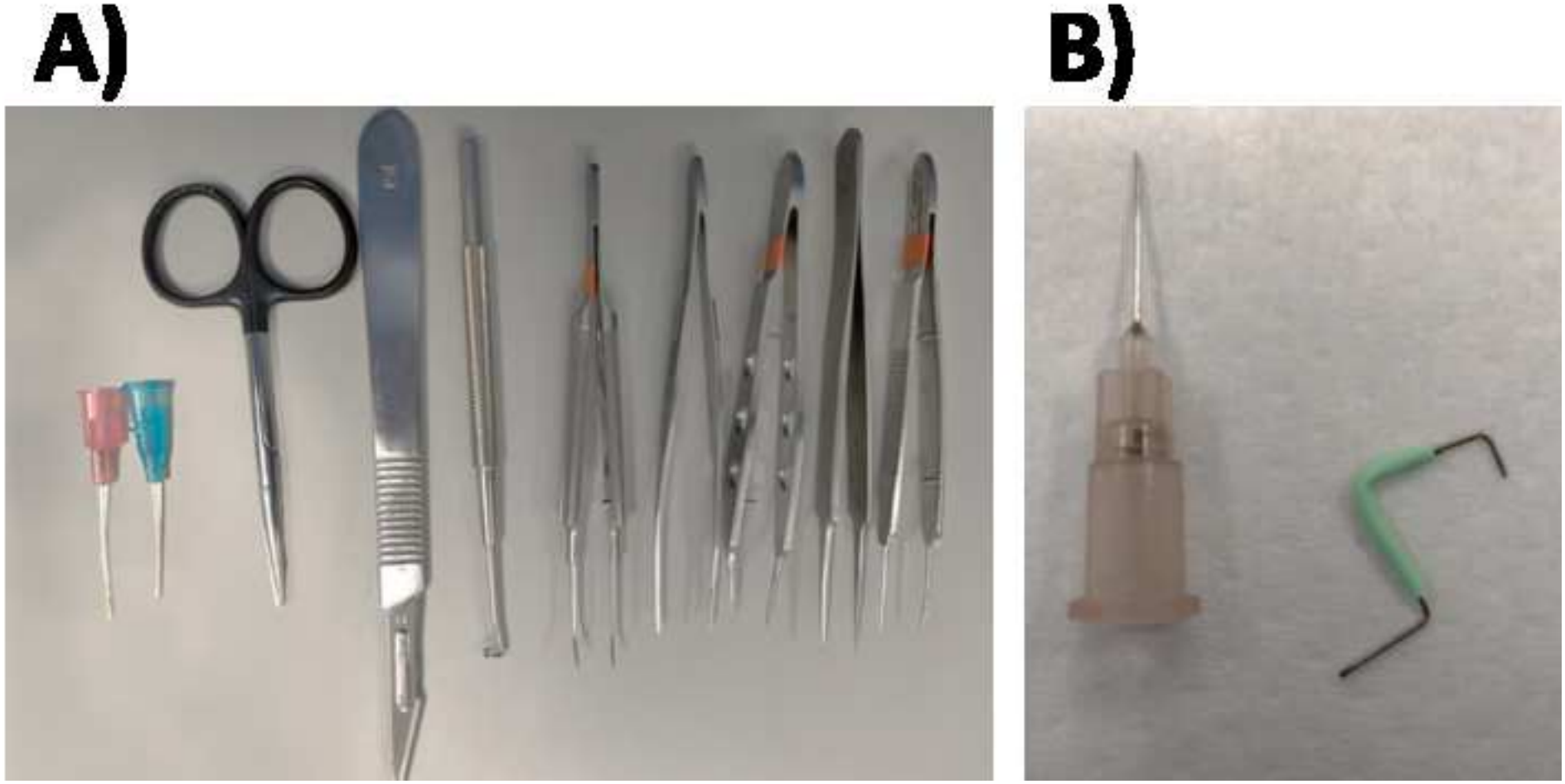

Figure 2

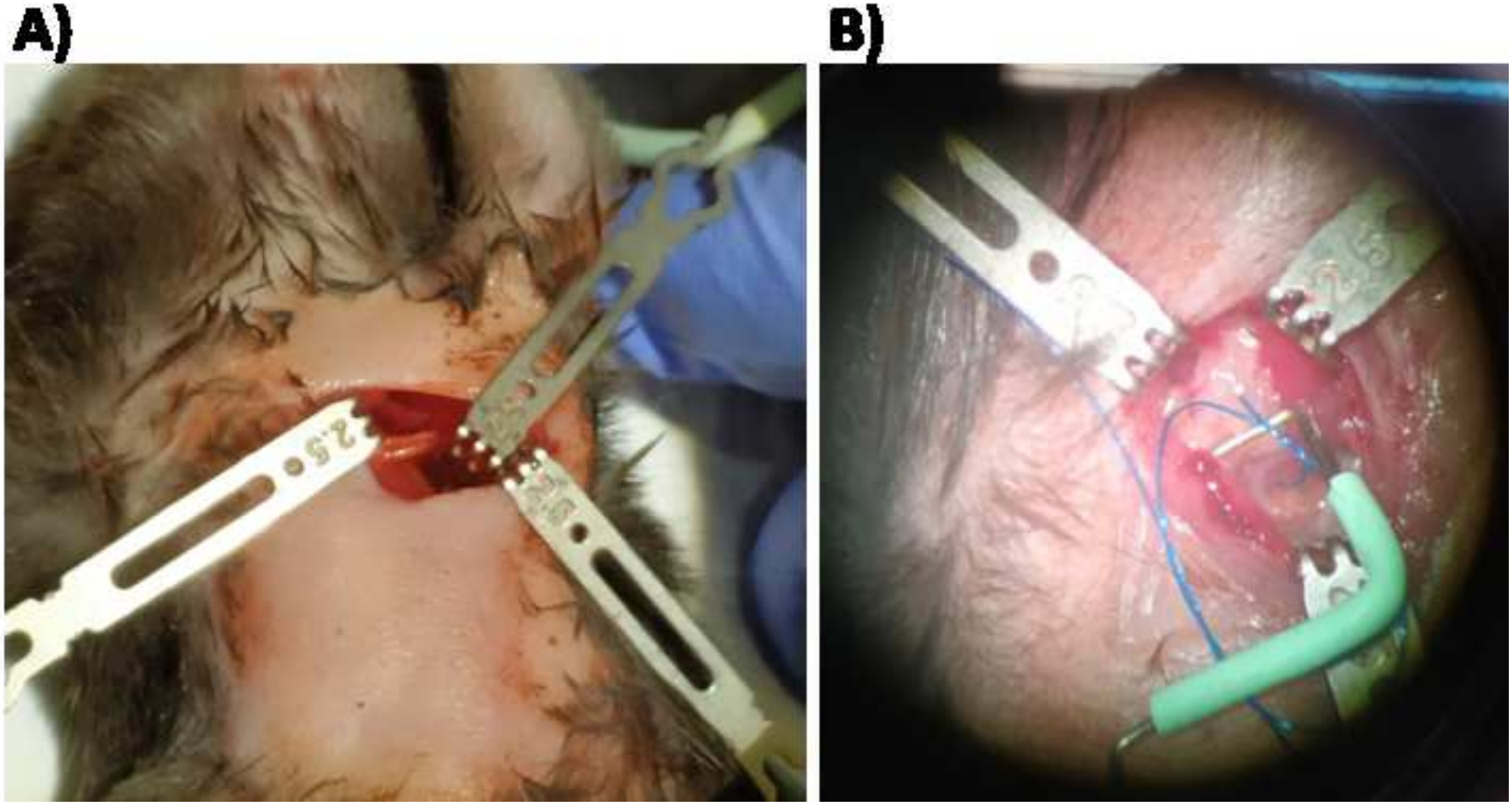

Figure 3

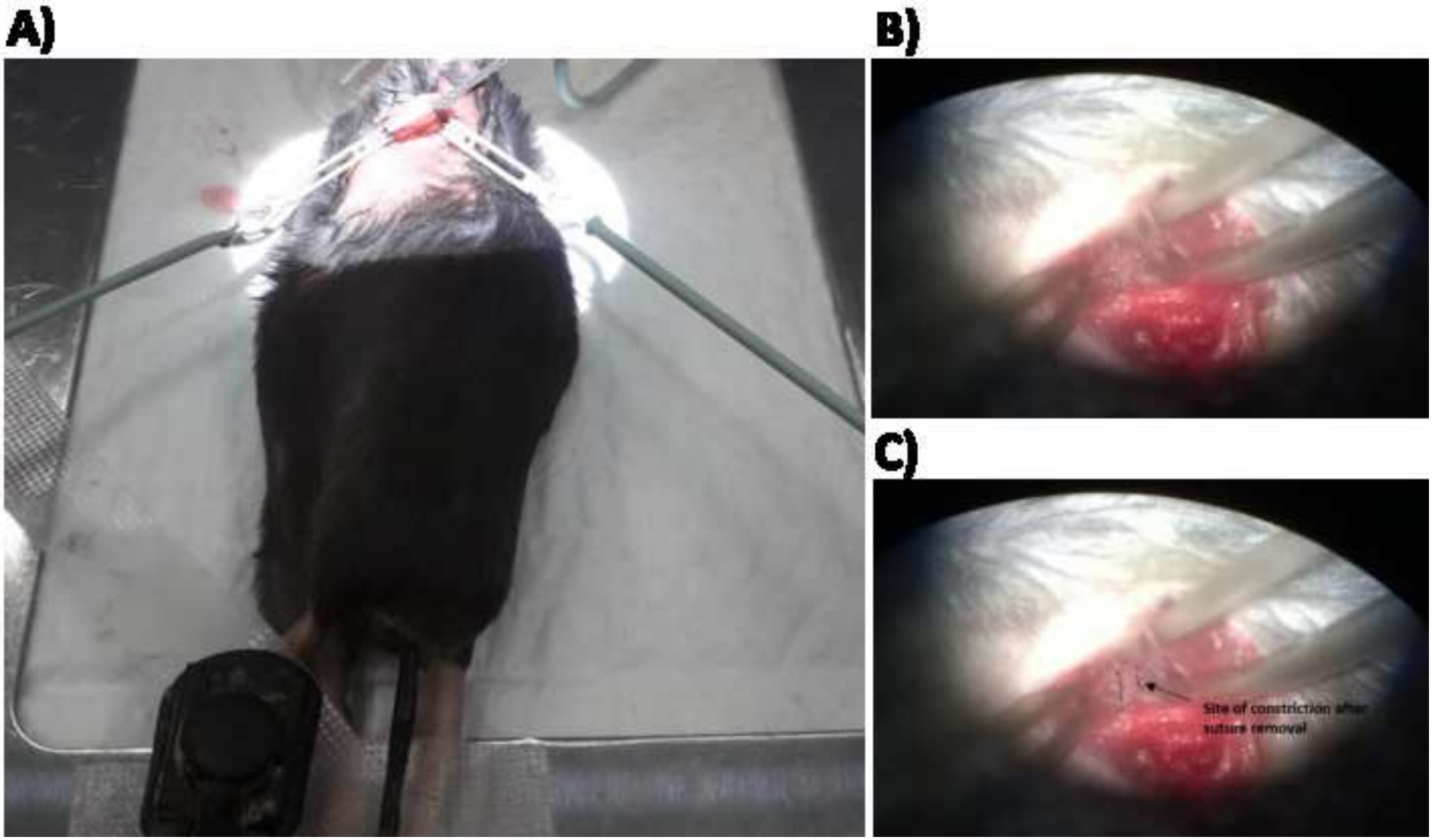

Figure 4

Click here to access/download;Figure;Image4.png

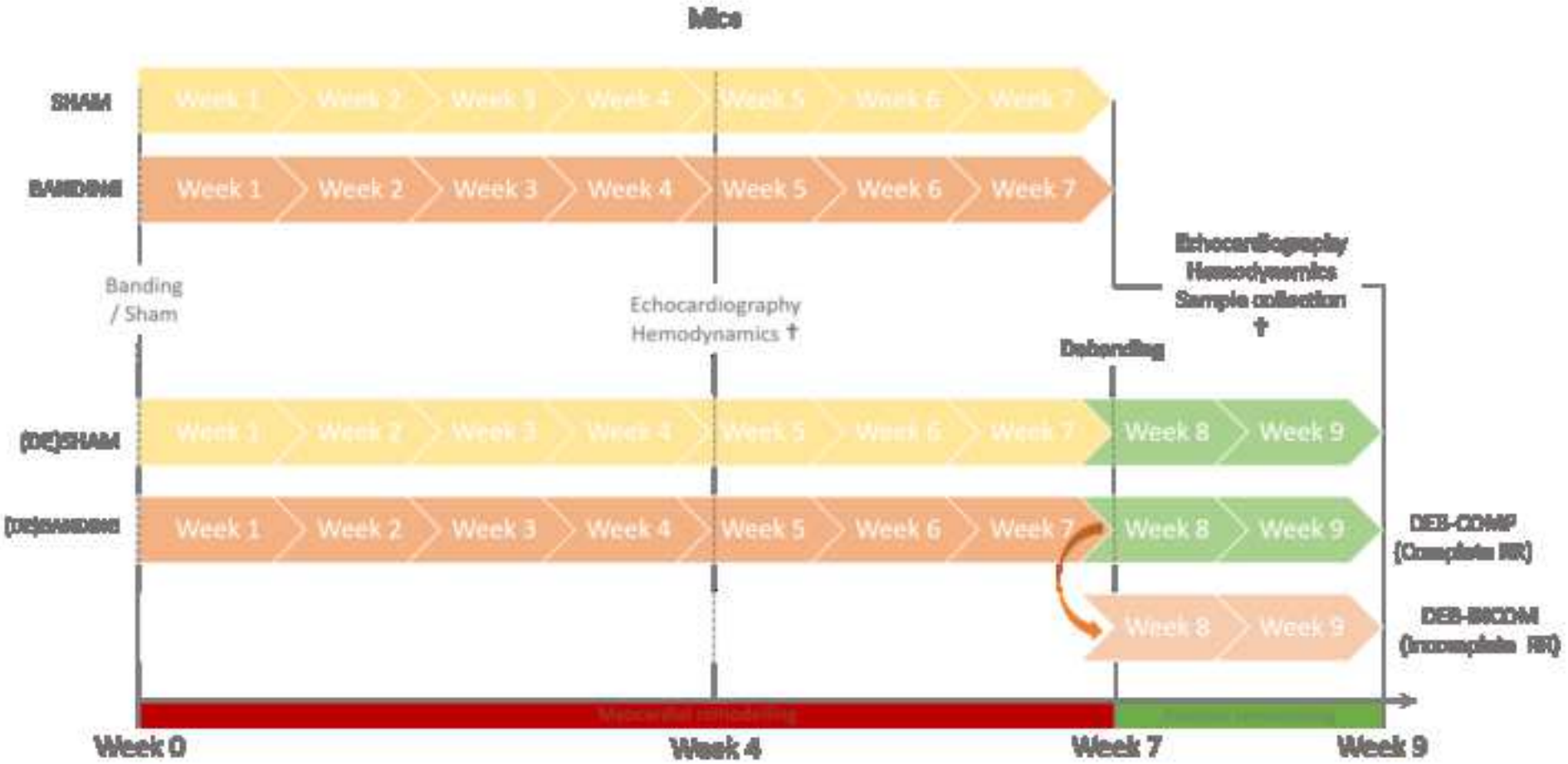

Figure 5

Click here to access/download;Figure;Image5 (1).png

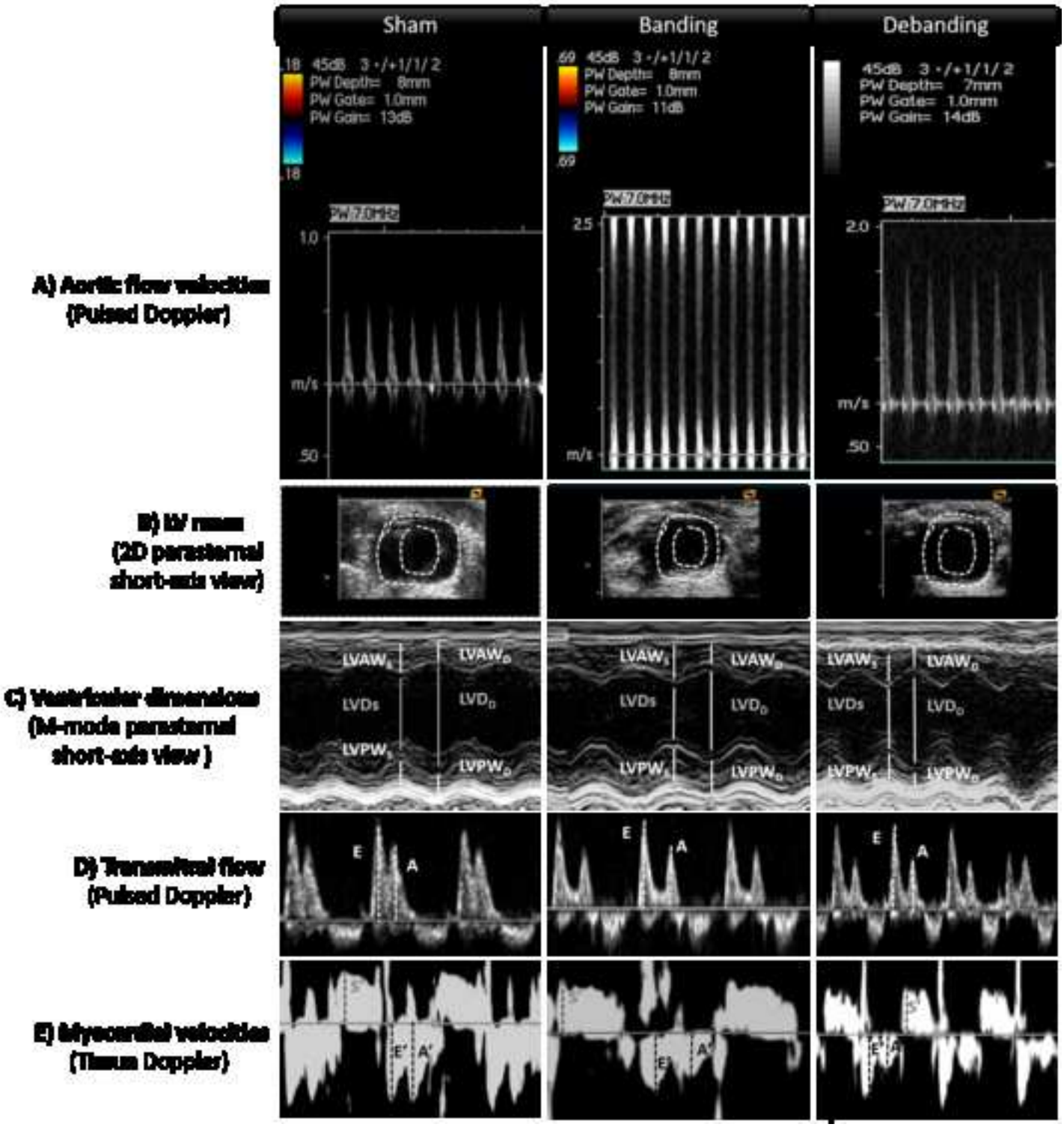

Figure 6

Click here to access/download;Figure;Image6.png

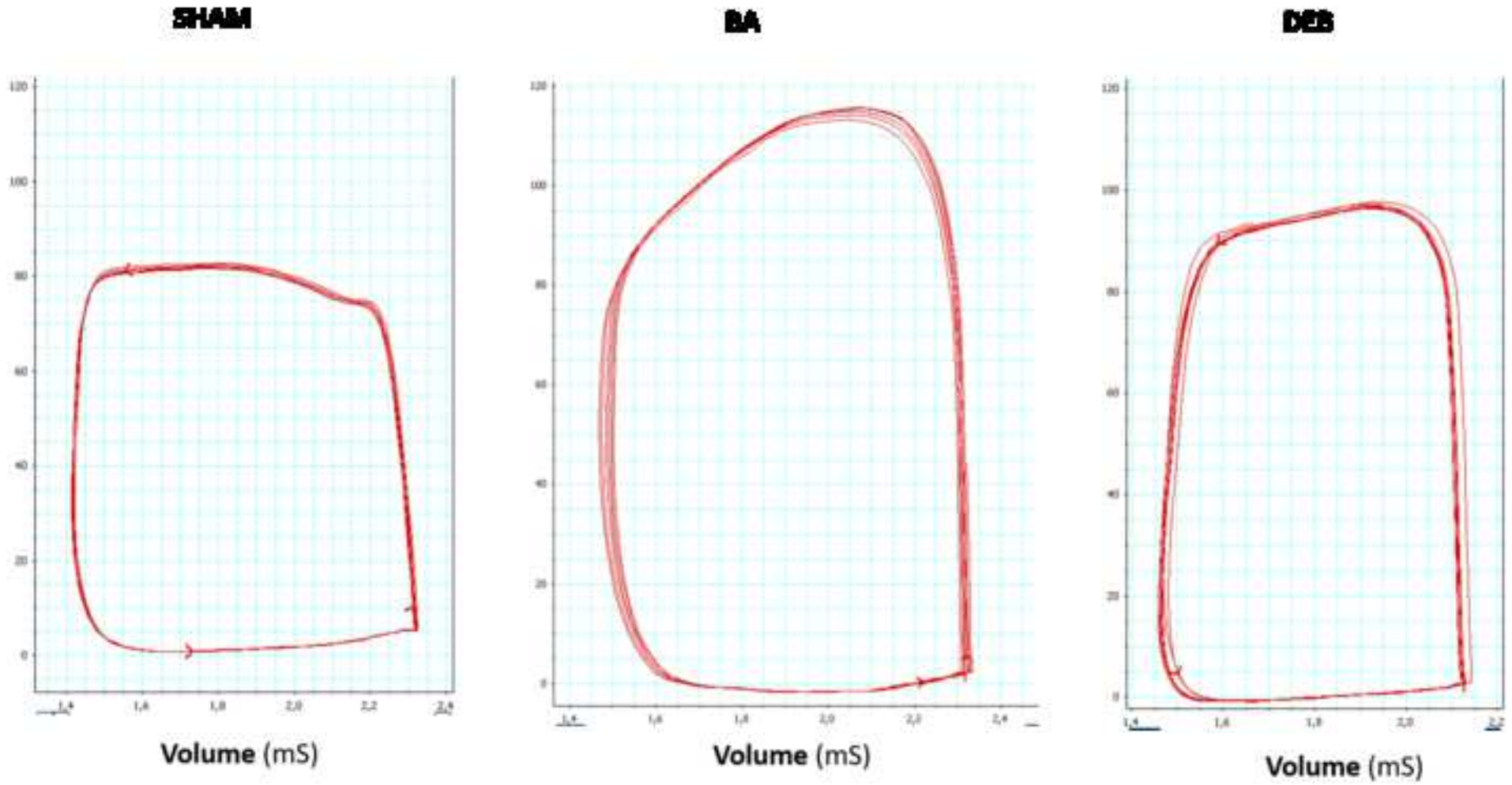

Figure 7

Click here to access/download;Figure;Image7.png

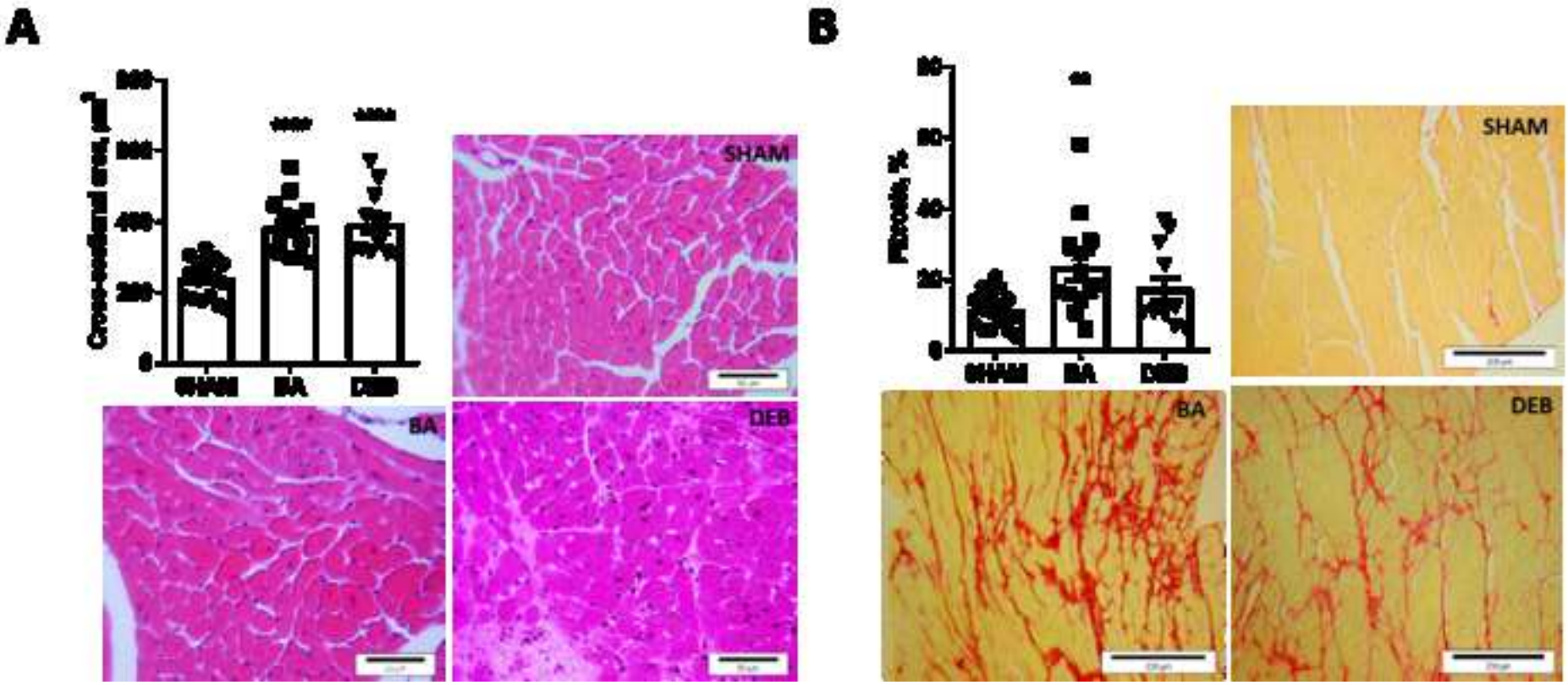

Table 1. Morphological and functional data

	SHAM (n=19)	BA (n=15)	DEB (n=14)
Body weight (mg)	28.07±0.34	27.57±0.58	26.72±0.65
Heart weight/BSA (mg/cm^2)	74.28±2.19	103.00±9.84$^{\alpha\alpha}$	84.04±3.47
LV Mass (mg/cm^2)	1.23±0.06	1.80±0.11$^{\alpha\alpha\alpha\alpha}$	1.39±0.12$^{\chi\chi}$
EDVI (uL/cm^2)	0.78±0.04	0.84±0.07	0.79±0.07
ESVI (uL/cm^2)	0.32±0.02	0.33±0.04	0.34±0.04
E/E'	13.81±0.61	20.44±1.51$^{\alpha\alpha\alpha}$	14.81±1.22$^{\chi\chi}$
E/A	1.46±0.06	1.59±0.08	1.57±0.12
S´	0.041±0.003	0.049±0.010	0.036±0.003
EF (%)	58.16±2.11	61.87±2.93	58.63±3.77
LVSP (mmHg)	80.79 ± 3.97	107.20 ± 7.84$^{\alpha\alpha}$	88.63 ± 3.87
LVEDP (mmHg)	4.79 ± 0.75	9.77 ± 2.37$^{\alpha}$	3.94 ± 0.45$^{\chi\chi}$
HR (bpm)	523 ± 16	466 ± 25	529± 17
Tau (ms)	5.77 ± 0.34	9.79 ± 2.86	6.00 ± 0.43

Table 2

Critical steps
Invasiveness of the banding surgery
Suture internalization
Physiological parameters

Advice

It is important to avoid:

- prolonged occlusion of the ascending aorta during the ligation, which may lead to lung edema and activation of inflammatory pathways capable of influencing the phenotype and disease severity[15];
- bleeding of the mammary artery which, if not timely circumvented, can lead to decreased blood pressure and promote higher amounts of fibrosis when re-opening the thorax (debanding);
- damaging mice pleura and lungs;

Mini left lateral thoracotomy for banding and debanding (same place; present study) vs left lateral thoracotomy for the banding and a sternotomy for the debanding surgery[11]:

- the first is less invasive and have a short-recovery time, which improves the success of the open-chest haemodynamic performed two weeks later. Neverthless, the use of same position to re-open the chest can increase the number of complications due to adhesions (around left atrium, pulmonary artery, etc).

Can be prevented by using:

- two banding sutures side-by-side[16];
- silk instead of polypropylene[11]**;**
- titanium clips or a O-rings around the aorta to induce its constriction [21];
- double loop-clip thecnique[15];
- inflatable cuff to carry out supracoronary aortic banding[22].

During surgery it is important to monitor:

- heart rate;
- blood oxygenation, keeping it above 90% (specially during aorta manupilation);
- anesthesia, keeping it at the lowest dose possible without inflicting discomfort on the animal.

Name of Material/Equipment	Company	Catalog Number
Absorption Spears	F.S.T	18105-03
Blades	F.S.T	10011-00
Buprenorphine	Buprelieve	
Catutery	F.S.T	18010-00
Catutery tips	F.S.T	18010-01
cotton swab	Johnson's	
Depilatory cream	Veet	
Disposable operating room table cover	MEDKINE	DYND4030SB
Echo probe	Siemens	Sequoia 15L8W
Echocardiograph	Siemens	*Acuson Sequoia* C512
End-tidal CO_2 monitor	Kent Scientific	CapnoStat
Forcep/Tweezers	F.S.T	11255-20
Forcep/Tweezers	F.S.T	11272-30
Forcep/Tweezers	F.S.T	11151-10
Forcep/Tweezers	F.S.T	11152-10
Gas system	Penlon Sigma Delta	
Hemostats	F.S.T	13010-12
Hemostats	F.S.T	13011-12
Ligation aids	F.S.T	18062-12
Magnetic retractor	F.S.T	18200-20
Needle holder	F.S.T	12503-15
Needle 26G	B-BRAUN	4665457
Oxygen	Air Liquide	
Polipropilene suture	Vycril	W8304/W8597
Povidone-iodine solution	Betadine®	
PowerLab	Millar instruments	ML880 PowerLab 16/30
Pulse oximeter	Kent Scientific	MouseStat
PVAN software	Millar Instruments	
PV loop cathether	Millar instruments	SPR-*1035* . 1.4 F
Retractor	F.S.T	17000-01
Scalpet handle	F.S.T	10003-12

Scissors	F.S.T	15070-08
Scissors	F.S.T	14084-09
Sevoflurane	Baxter	533-CA2L9117
Temperature control module	Kent Scientific	RightTemp
Ventilator	Kent Scientific	PhysioSuite
Water-bath	Thermo Scientific™	TSGP02

Comments/Description
To absorb fluids during the surgery
To perform the skin incision
Analgesia drug
To prevent exsanguination
To prevent exsanguination
To absorb fluids during the surgery
To delipate the animal
To cover the surgical area
Ultrasound signal aquisition
Ultrasound signal aquisition
To control expiration gas saturation
To dissect the tissues and aorta
To dissect the tissues and aorta
To dissect the tissues and aorta
To dissect the tissues and aorta
To anesthesia and mechanical ventilation
To hold the suture before tight the aorta
To hold the suture before tight the aorta
To place a suture around the aorta
To help keep the animal in a proper position
To suture the animal
To serve as a molde of aortic constriction diameter
To anesthesia and mechanical ventilation
To suture the animal and to do the constriction
Skin antiseptic
PV loop Signal Aquisition
To control heart rate and blood saturation
To analyse the haemodynamic data
PV loop Signal Aquisition
To provide a better overview of the aorta
To perform the skin incision

To cut the suture in debanding surgery

To cut other material during the surgery e.g. suture, papper

To control animal corporal temperature

To ventilate the animal

naintain water temperature adequate to heat the P-V loop catethers

jove JOURNAL OF VISUALIZED EXPERIMENTS
1 Alewife Center #200
Cambridge, MA 02140
tel. 617.945.9051
www.jove.com

ARTICLE AND VIDEO LICENSE AGREEMENT

Title of Article: AORTIC DEBANDING AS A VALUABLE RODENT MODEL FOR STUDYING LV RR

Author(s): PATRICIA GONÇALVES-RODRIGUES, DANIELA MIRANDA-SILVA, ADELINO F LEITE-MOREIRA, INÊS FALCÃO-PIRES

Item 1: The Author elects to have the Materials be made available (as described at http://www.jove.com/publish) via:

☒ Standard Access ☐ Open Access

Item 2: Please select one of the following items:

☒ The Author is **NOT** a United States government employee.

☐ The Author is a United States government employee and the Materials were prepared in the course of his or her duties as a United States government employee.

☐ The Author is a United States government employee but the Materials were NOT prepared in the course of his or her duties as a United States government employee.

ARTICLE AND VIDEO LICENSE AGREEMENT

1. **Defined Terms.** As used in this Article and Video License Agreement, the following terms shall have the following meanings: "**Agreement**" means this Article and Video License Agreement; "**Article**" means the article specified on the last page of this Agreement, including any associated materials such as texts, figures, tables, artwork, abstracts, or summaries contained therein; "**Author**" means the author who is a signatory to this Agreement; "**Collective Work**" means a work, such as a periodical issue, anthology or encyclopedia, in which the Materials in their entirety in unmodified form, along with a number of other contributions, constituting separate and independent works in themselves, are assembled into a collective whole; "**CRC License**" means the Creative Commons Attribution-Non Commercial-No Derivs 3.0 Unported Agreement, the terms and conditions of which can be found at: http://creativecommons.org/licenses/by-nc-nd/3.0/legalcode; "**Derivative Work**" means a work based upon the Materials or upon the Materials and other pre-existing works, such as a translation, musical arrangement, dramatization, fictionalization, motion picture version, sound recording, art reproduction, abridgment, condensation, or any other form in which the Materials may be recast, transformed, or adapted; "**Institution**" means the institution, listed on the last page of this Agreement, by which the Author was employed at the time of the creation of the Materials; "**JoVE**" means MyJove Corporation, a Massachusetts corporation and the publisher of The Journal of Visualized Experiments; "**Materials**" means the Article and / or the Video; "**Parties**" means the Author and JoVE; "**Video**" means any video(s) made by the Author, alone or in conjunction with any other parties, or by JoVE or its affiliates or agents, individually or in collaboration with the Author or any other parties, incorporating all or any portion of the Article, and in which the Author may or may not appear.

2. **Background.** The Author, who is the author of the Article, in order to ensure the dissemination and protection of the Article, desires to have the JoVE publish the Article and create and transmit videos based on the Article. In furtherance of such goals, the Parties desire to memorialize in this Agreement the respective rights of each Party in and to the Article and the Video.

3. **Grant of Rights in Article.** In consideration of JoVE agreeing to publish the Article, the Author hereby grants to JoVE, subject to **Sections 4** and **7** below, the exclusive, royalty-free, perpetual (for the full term of copyright in the Article, including any extensions thereto) license (a) to publish, reproduce, distribute, display and store the Article in all forms, formats and media whether now known or hereafter developed (including without limitation in print, digital and electronic form) throughout the world, (b) to translate the Article into other languages, create adaptations, summaries or extracts of the Article or other Derivative Works (including, without limitation, the Video) or Collective Works based on all or any portion of the Article and exercise all of the rights set forth in (a) above in such translations, adaptations, summaries, extracts, Derivative Works or Collective Works and(c) to license others to do any or all of the above. The foregoing rights may be exercised in all media and formats, whether now known or hereafter devised, and include the right to make such modifications as are technically necessary to exercise the rights in other media and formats. If the "Open Access" box has been checked in **Item 1** above, JoVE and the Author hereby grant to the public all such rights in the Article as provided in, but subject to all limitations and requirements set forth in, the CRC License.

jove JOURNAL OF VISUALIZED EXPERIMENTS
1 Alewife Center #200
Cambridge, MA 02140
tel. 617.945.9051
www.jove.com

ARTICLE AND VIDEO LICENSE AGREEMENT

4. **Retention of Rights in Article.** Notwithstanding the exclusive license granted to JoVE in **Section 3** above, the Author shall, with respect to the Article, retain the non-exclusive right to use all or part of the Article for the non-commercial purpose of giving lectures, presentations or teaching classes, and to post a copy of the Article on the Institution's website or the Author's personal website, in each case provided that a link to the Article on the JoVE website is provided and notice of JoVE's copyright in the Article is included. All non-copyright intellectual property rights in and to the Article, such as patent rights, shall remain with the Author.

5. **Grant of Rights in Video – Standard Access.** This **Section 5** applies if the "Standard Access" box has been checked in **Item 1** above or if no box has been checked in **Item 1** above. In consideration of JoVE agreeing to produce, display or otherwise assist with the Video, the Author hereby acknowledges and agrees that, Subject to **Section 7** below, JoVE is and shall be the sole and exclusive owner of all rights of any nature, including, without limitation, all copyrights, in and to the Video. To the extent that, by law, the Author is deemed, now or at any time in the future, to have any rights of any nature in or to the Video, the Author hereby disclaims all such rights and transfers all such rights to JoVE.

6. **Grant of Rights in Video – Open Access.** This **Section 6** applies only if the "Open Access" box has been checked in **Item 1** above. In consideration of JoVE agreeing to produce, display or otherwise assist with the Video, the Author hereby grants to JoVE, subject to **Section 7** below, the exclusive, royalty-free, perpetual (for the full term of copyright in the Article, including any extensions thereto) license (a) to publish, reproduce, distribute, display and store the Video in all forms, formats and media whether now known or hereafter developed (including without limitation in print, digital and electronic form) throughout the world, (b) to translate the Video into other languages, create adaptations, summaries or extracts of the Video or other Derivative Works or Collective Works based on all or any portion of the Video and exercise all of the rights set forth in (a) above in such translations, adaptations, summaries, extracts, Derivative Works or Collective Works and (c) to license others to do any or all of the above. The foregoing rights may be exercised in all media and formats, whether now known or hereafter devised, and include the right to make such modifications as are technically necessary to exercise the rights in other media and formats. For any Video to which this **Section 6** is applicable, JoVE and the Author hereby grant to the public all such rights in the Video as provided in, but subject to all limitations and requirements set forth in, the CRC License.

7. **Government Employees.** If the Author is a United States government employee and the Article was prepared in the course of his or her duties as a United States government employee, as indicated in **Item 2** above, and any of the licenses or grants granted by the Author hereunder exceed the scope of the 17 U.S.C. 403, then the rights granted hereunder shall be limited to the maximum rights permitted under such statute. In such case, all provisions contained herein that are not in conflict with such statute shall remain in full force and effect, and all provisions contained herein that do so conflict shall be deemed to be amended so as to provide to JoVE the maximum rights permissible within such statute.

8. **Protection of the Work.** The Author(s) authorize JoVE to take steps in the Author(s) name and on their behalf if JoVE believes some third party could be infringing or might infringe the copyright of either the Author's Article and/or Video.

9. **Likeness, Privacy, Personality.** The Author hereby grants JoVE the right to use the Author's name, voice, likeness, picture, photograph, image, biography and performance in any way, commercial or otherwise, in connection with the Materials and the sale, promotion and distribution thereof. The Author hereby waives any and all rights he or she may have, relating to his or her appearance in the Video or otherwise relating to the Materials, under all applicable privacy, likeness, personality or similar laws.

10. **Author Warranties.** The Author represents and warrants that the Article is original, that it has not been published, that the copyright interest is owned by the Author (or, if more than one author is listed at the beginning of this Agreement, by such authors collectively) and has not been assigned, licensed, or otherwise transferred to any other party. The Author represents and warrants that the author(s) listed at the top of this Agreement are the only authors of the Materials. If more than one author is listed at the top of this Agreement and if any such author has not entered into a separate Article and Video License Agreement with JoVE relating to the Materials, the Author represents and warrants that the Author has been authorized by each of the other such authors to execute this Agreement on his or her behalf and to bind him or her with respect to the terms of this Agreement as if each of them had been a party hereto as an Author. The Author warrants that the use, reproduction, distribution, public or private performance or display, and/or modification of all or any portion of the Materials does not and will not violate, infringe and/or misappropriate the patent, trademark, intellectual property or other rights of any third party. The Author represents and warrants that it has and will continue to comply with all government, institutional and other regulations, including, without limitation all institutional, laboratory, hospital, ethical, human and animal treatment, privacy, and all other rules, regulations, laws, procedures or guidelines, applicable to the Materials, and that all research involving human and animal subjects has been approved by the Author's relevant institutional review board.

11. **JoVE Discretion.** If the Author requests the assistance of JoVE in producing the Video in the Author's facility, the Author shall ensure that the presence of JoVE employees, agents or independent contractors is in accordance with the relevant regulations of the Author's institution. If more than one author is listed at the beginning of this Agreement, JoVE may, in its sole

jove JOURNAL OF VISUALIZED EXPERIMENTS
1 Alewife Center #200
Cambridge, MA 02140
tel. 617.945.9051
www.jove.com

ARTICLE AND VIDEO LICENSE AGREEMENT

discretion, elect not take any action with respect to the Article until such time as it has received complete, executed Article and Video License Agreements from each such author. JoVE reserves the right, in its absolute and sole discretion and without giving any reason therefore, to accept or decline any work submitted to JoVE. JoVE and its employees, agents and independent contractors shall have full, unfettered access to the facilities of the Author or of the Author's institution as necessary to make the Video, whether actually published or not. JoVE has sole discretion as to the method of making and publishing the Materials, including, without limitation, to all decisions regarding editing, lighting, filming, timing of publication, if any, length, quality, content and the like.

12. **Indemnification.** The Author agrees to indemnify JoVE and/or its successors and assigns from and against any and all claims, costs, and expenses, including attorney's fees, arising out of any breach of any warranty or other representations contained herein. The Author further agrees to indemnify and hold harmless JoVE from and against any and all claims, costs, and expenses, including attorney's fees, resulting from the breach by the Author of any representation or warranty contained herein or from allegations or instances of violation of intellectual property rights, damage to the Author's or the Author's institution's facilities, fraud, libel, defamation, research, equipment, experiments, property damage, personal injury, violations of institutional, laboratory, hospital, ethical, human and animal treatment, privacy or other rules, regulations, laws, procedures or guidelines, liabilities and other losses or damages related in any way to the submission of work to JoVE, making of videos by JoVE, or publication in JoVE or elsewhere by JoVE. The Author shall be responsible for, and shall hold JoVE harmless from, damages caused by lack of sterilization, lack of cleanliness or by contamination due to the making of a video by JoVE its employees, agents or independent contractors. All sterilization, cleanliness or decontamination procedures shall be solely the responsibility of the Author and shall be undertaken at the Author's expense. All indemnifications provided herein shall include JoVE's attorney's fees and costs related to said losses or damages. Such indemnification and holding harmless shall include such losses or damages incurred by, or in connection with, acts or omissions of JoVE, its employees, agents or independent contractors.

13. **Fees.** To cover the cost incurred for publication, JoVE must receive payment before production and publication of the Materials. Payment is due in 21 days of invoice. Should the Materials not be published due to an editorial or production decision, these funds will be returned to the Author. Withdrawal by the Author of any submitted Materials after final peer review approval will result in a US$1,200 fee to cover pre-production expenses incurred by JoVE. If payment is not received by the completion of filming, production and publication of the Materials will be suspended until payment is received.

14. **Transfer, Governing Law.** This Agreement may be assigned by JoVE and shall inure to the benefits of any of JoVE's successors and assignees. This Agreement shall be governed and construed by the internal laws of the Commonwealth of Massachusetts without giving effect to any conflict of law provision thereunder. This Agreement may be executed in counterparts, each of which shall be deemed an original, but all of which together shall be deemed to me one and the same agreement. A signed copy of this Agreement delivered by facsimile, e-mail or other means of electronic transmission shall be deemed to have the same legal effect as delivery of an original signed copy of this Agreement.

A signed copy of this document must be sent with all new submissions. Only one Agreement is required per submission.

CORRESPONDING AUTHOR

Name:	Inês Falcão - Pires
Department:	Unidade de Investigação Cardiovascular, Departamento de Cirurgia e Fisiologia, Faculdade de Medicina da Universidade do Porto
Institution:	Faculdade de Medicina da Universidade do Porto
Title:	Assistant Professor
Signature:	Inês Falcão Pires
Date:	20/03/2019

Please submit a **signed** and **dated** copy of this license by one of the following three methods:

1. Upload an electronic version on the JoVE submission site
2. Fax the document to +1.866.381.2236
3. Mail the document to JoVE / Attn: JoVE Editorial / 1 Alewife Center #200 / Cambridge, MA 02140

Dear editor:

Please find enclosed the revised version of the manuscript entitled “AORTIC DEBANDING AS A VALUABLE RODENT MODEL FOR STUDYING LEFT VENTRICULAR REVERSE REMODELING” by Patrícia Goncalves-Rodrigues, Daniela Miranda-Silva, Adelino F Leite-Moreira and Inês Falcão-Pires.

We thank the reviewers for their brilliant and detailed analysis of our work, which helped us to improve the manuscript. All the points raised by the reviewers were taken into account, and the manuscript was corrected accordingly ("track changes” in red, pule and in blue). Furthermore, we include below an answer where we outline, point by point, each change made as raised in the editor or reviewers’ comments. We sincerely believe that the revised version will comply with their suggestions.

Editorial comments:

Changes to be made by the Author(s):

1. Please take this opportunity to thoroughly proofread the manuscript to ensure that there are no spelling or grammar issues. The JoVE editor will not copy-edit your manuscript and any errors in the submitted revision may be present in the published version.

We asked a native English speaker to revise the entire manuscript, and we hope this version is significantly improved.

2. Please define all abbreviations during the first-time use.

We have confirmed all the abbreviations.

3. Please remove all commercial language from your manuscript and use generic terms instead. All commercial products should be sufficiently referenced in the Table of Materials and Reagents. For example: Charles River, Spain, Fine Science Tools, Penlon Sigma Delta, TOPO Small Animal Ventilator, Kent Scientific Inc., vycril, SPR-1035. 1.4 F, Millar instruments, (MPVS 300, Millar Instruments, ML880 PowerLab 16/30, 241 Millar Instruments, etc

4. Please include a single line space between each step, substep and note in the protocol section.

We have done so and send all important information to the Table od Materials and Reagents.

5. Please ensure that all text in the protocol section is written in the imperative tense as if

telling someone how to do the technique (e.g., “Do this,” “Ensure that,” etc.). The actions should be described in the imperative tense in complete sentences wherever possible. Avoid usage of phrases such as “could be,” “should be,” and “would be” throughout the Protocol. Any text that cannot be written in the imperative tense may be added as a “Note.” However, notes should be concise and used sparingly.

6. The Protocol should contain only action items that direct the reader to do something.
7. Please add more details to your protocol steps. Please ensure you answer the “how” question, i.e., how is the step performed? For example, see below:
8. Lines 108-111: This can be converted to a note and the materials required can be moved to the materials table.

We have addressed all these remarks and significantly changed the methods to include action sentences (imperative tense) explained in more detail. Some parts of the text were converted to CRITICAL STEPS and NOTES.

9. 3.1: Do you check the depth of anesthesia?

10. 3.2: How is this done?

11. 3.6: Need more details on thoracotomy.

12. For all substeps in 3: Please include how is this done? Using what instrument?

13. 4, 5, 6, 7,8: Include how?

We always monitor anesthesia depth by checking the toe-pinch reflex. This information has been added to the revised version of the manuscript. We also added and clarified the details of thoracotomy and all the substeps of 3 (now 4).

14. 5.2: Step 2.6 is not present. Please check the step numbers.

All the step numbers have been reviewed.

15. Software steps must be more explicitly explained ('click', 'select', etc.). Please add more specific details (e.g. button clicks for software actions, numerical values for settings, etc.).
16. The Protocol should be made up almost entirely of discrete steps without large paragraphs of text between sections.

In the revised version of the manuscript, software steps were detailed and the long paragraphs in the method section were replaced by discrete and short sentences reporting to direct actions.

17. There is a 10-page limit for the Protocol, but there is a 2.75-page limit for filmable content. Please highlight 2.75 pages or less of the Protocol (including headings and spacing)

that identifies the essential steps of the protocol for the video, i.e., the steps that should be visualized to tell the most cohesive story of the Protocol.

We have highlighted in green the filmable content identifying the essential steps for the video protocol.

18. Please obtain explicit copyright permission to reuse any figures from a previous publication. Explicit permission can be expressed in the form of a letter from the editor or a link to the editorial policy that allows re-prints. Please upload this information as a .doc or .docx file to your Editorial Manager account. The Figure must be cited appropriately in the Figure Legend, i.e. "This figure has been modified from [citation]."

There are no figures from previous publications.

19. As we are a methods journal, please revise the Discussion to explicitly cover the following in detail in 3-6 paragraphs with citations:

a) Critical steps within the protocol

b) Any modifications and troubleshooting of the technique

c) Any limitations of the technique

d) The significance with respect to existing methods

e) Any future applications of the technique

The discussion has been dramatically reduced:

1. *We created a table (Table 2) to summarise the critical steps and remove this information from the text.*
2. *We removed an entire paragraph related to the aortic constriction procedure. Since we consider the focus of this paper to be the aortic debanding, rather than the banding procedure, we excluded this paragraph.*
3. *An effort was made to keep the most relevant information and the topics a, b, c, d and e mentioned above by the editor.*

However, in order to address some reviewers' comments, we add some text to the discussion. So, if the editor finds interesting, we could transform the paragraph highlighting the changes between mice and rats into a table.

20. Please ensure that the references appear as the following: [Lastname, F.I., LastName, F.I., LastName, F.I. Article Title. Source. Volume (Issue), FirstPage – LastPage, (YEAR).] For more than 6 authors, list only the first author then et al. Please do not abbreviate the journal title.

21. Please remove the legends from the figures.

22. Figure 1,6: Please hide the commercial name: Prolene, Miller

23. Please revise the table of the essential supplies, reagents, and equipment. The table should include the name, company, and catalog number of all relevant materials in separate columns in an xls/xlsx file. Please alphabetically sort the materials table.

The material table has been updated according to the editor suggestions.

Reviewers' comments:

Reviewer #1:

In this methodological paper, Falcao Pires et al. has given a proper description of a rodent model of ascending aortic constriction-induced myocardial remodeling and debanding-evoked reverse remodeling. The subject of the presented manuscript (pressure overload-induced remodeling and pressure unloading-induced reverse remodeling) is currently a central issue in the field of cardiovascular medicine and animal models similar to that was described in the present study represent an adequate tool to mimic those alterations that occur after aortic valve replacement therapy (surgical or transcatheter). The description of the utilized model is adequate and the notes related to this model are important/helpful. The following comments should be addressed before accepting the manuscript for publication.

We thank the reviewer for the valuable remarks.

Comment 1: Fibrosis.

The authors claim in the introduction that myocardial fibrosis is irreversible after pressure unloading therapy. However, it is important to note that myocardial fibrosis can be subdivided into replacement and reactive fibrosis. Previous clinical studies have demonstrated that replacement fibrosis is indeed unable to regress. However, recent studies utilizing novel cardiac magnetic resonance imaging have revealed that reactive, diffuse fibrosis (including interstitial and perivascular fibrosis) is able to regress in the long term.

We agree with the reviewer comment. We added this information in the introduction (line 65 to 71).

Comment 2: Pressure-volume analysis.

The authors used an open chest pressure-volume (P-V) analysis method to assess left ventricular hemodynamics. Nevertheless, the closed chest P-V analysis technique (when the catheter is guided from the right carotid artery into the left ventricle) would be another solution. Is the closed chest technique feasible in ascending aortic constricted mice? If not, it should be mentioned as a limitation.

The close-chest approach to perform hemodynamic evaluation is a much more conservative approach and, often, preferable over the open-chest approach. However, in the particular case of ascending aorta constriction, the insertion of the catheter into the left ventricle through the carotid is not feasible due to the location of the banding before the carotid branches. Furthermore, in rats, we use a flow probe to accurate cardiac output, which is considered the gold-standard technique and impossible to perform in a closed-chest approached. Therefore, following the reviewer suggestion, we included this limitation in the discussion section (line 509-512).

Furthermore, one of the main advantage of P-V analysis is the possibility to measure load-independent contractility (e.g. slope of ESPVR, PRSW) and diastolic parameters (slope of EDPVR) by performing vena cava occlusion maneuver. This is of particular interest in case of aortic constriction, when the robust alteration in afterload makes the conventional parameters inadequate to characterize myocardial function. Can the author comment on it, why did they not measure these particular parameters?

We agree with the reviewer and recognize that the absence of load-independent parameters may be a study limitation. Nevertheless, we feel that hemodynamic and its derived parameters are not the emphasis of the paper as these represent a way to assess the cardiac function of the mice model of debanding, which is the focus of the paper. We did not perform these maneuvers because in mice we were not able to measure cardiac output and thus we could not do the alpha correction to transform conductance into volume (mL). In rats, this limitation does not exist as by placing the flow probe around the aorta it is easy to have cardiac output and thus work with the correct volumes. We include this as a limitation of the study (line 512-517).

The authors named LVEDP as an index of left ventricular stiffness, which is not 100% correct. Correspondingly, LVEDP is a valuable parameter of passive filling. However, the slope of EDPVR is traditionally used to describe chamber stiffness.

We agree with the reviewer and changed the text accordingly (line 372).

The SPR-847 (1.4 F) catheter was suggested to fit the best in rats. However, our experience suggests that SPR-838 (2F) is the most suitable in a big range of rat size (body weight from 200 grams to 600 grams).

Both catheters are similar as they share the main characteristics, the key difference is the major effective length on SPR-838. However, the distance between the electrodes is the same (0.5 mm with the distance between each pair of 9.0 mm, pressure sensor placed between the two pairs of electrodes). In our opinion both catheters are adequate and both are widely used in the cardiovascular field in rats, beyond our laboratory[1, 2].

The authors suggest to use the femoral vein for vena cannulation in rats. However, I would like to stress it out that the left jugular vein should be used in most cases in rats as well. During the injection of saline boluses (for parallel conductance calculation) the substance should find its way quickly to the left ventricle. Therefore, the cannula is most often guided from the left jugular vein into the right atrium. This ensures that the saline bolus immediately (after going through the pulmonary circulation) reaches the left ventricle.

The reviewer is correct. In fact, in our laboratory, different users are more skilled to catheterize each one of these three possible veins, directly into the paw, femoral or jugular vein. For obvious anatomic reasons when the jugular vein is cannulated the saline bolus circuit is smaller. However, to the best of our knowledge, the magnitude of the differences is not enough to interfere with the results. Furthermore, we used the same approach during an entire protocol and the same amount of saline bolus (to better control the blood hyperconductivity).

P-V derived LVESP was utilized to measure the afterload. However, P-V analysis makes it possible to calculate arterial elastance (an integrative parameter of arterial afterload) which would probably give a more appropriate estimation of afterload.

We added this information to the table1 in the manuscript.

Comment 3: Time course.

The clinical experience suggest that reverse remodeling occurs in two phases. Early after AVR/TAVI, regression of cardiomyocyte hypertrophy takes place. However, reactive fibrosis often regresses only in the long term. Therefore, an additional group would be of particular interest when reverse remodeling is assessed after a longer follow-up period. The authors should comment on this issue.

We agree that it will be of interest to extend this time to understand the existence of these two phases and thus we included some sentences in the discussion addressing the translation of our animal model to clinical context (Line 475).

In mice, we only evaluated cardiac function after two weeks of RR. However, among DEB animals, we were able to separate two subgroups with distinct structural and functional phenotypes: DEB1 with persistently increased E/E' and fibrosis with LV mass regression; and DEB2 with E/E`, fibrosis and LV mass normalization. Both showing cardiomyocytes hypertrophy. Moreover, RNA sequence showed that DEB1 subgroup showed a higher number of dysregulated ECM related genes, which corroborates the phenotype findings (manuscript in preparation).

Comment 4: Echocardiography

The authors wrote that during echocardiographic measurement it is critical to maintain the heart rate over 300. Although, it is true I would suggest to give an even more strict range (e.g. between 300-350 beats/mind). According to my experience, substantial differences could be observed in left ventricular function in case of 300 and 400 beats/min as well.

We agree with the reviewer that heart rate has a profound impact on systolic and diastolic function. Nevertheless, in this particular case, as aortic banding induces a hypercontractile state, the reduction of heart rate to values similar between groups, will induce a strong cardiodepression in the banding group that will impact systolic and diastolic function, masking possible physiological differences among groups. We usually prefer to assess initially the heart rate of each animal under light anesthesia and then we try to stay close to those initial values.

Following the reviewer suggestion, we changed this in the paper (line 255).

Also on the representative captures demonstrating E/A ratio it is difficult to see the differences between sham and aortic banded rats. This should be improved.

In fact we did not found statistically differences amount groups on E/A ratio (as depicted in table1 and represented in the figure). Echocardiographycally the only diastolic parameter affected by aortic constriction was E/E', mainly due to myocardial hypocontractility.

Reviewer #2:

Manuscript Summary:

The manuscript describes a banding-debanding model of the aorta in mice (and rats). This is a technically challenging model and a video-illustration will be valuable for researchers wishing to establish this model to study reverse myocardial remodeling, in addition to the existing published descriptions.

We thank the reviewer for the valuable comments.

Major Concerns:

The authors recommend using a polypropylene suture for the aortic banding (7-0 in line 148 and 6-0 in line 308). The authors discuss the phenomenon of suture internalization (lines 361-371) as described by C. A. Lygate et al. (ref 15). In our similar publication (Bjørnstad JL, Skrbic B, Sjaastad I, Bjørnstad S, Christensen G, Tønnessen T. A mouse model of reverse cardiac remodelling following banding-debanding of the ascending aorta. Acta Physiol 2012;205:92-102), we also experienced this phenomenon and advocated the use of a silk suture. Even though the silk suture creates more scar tissue at the banding site, a more stable degree of pressure overload is achieved leaving at better starting-point before debanding to study reverse remodelling. Partial internalization of the polypropylene suture also increases the risk of fatal bleeding during debanding, and I would still recommend researchers to use a silk suture in a banding-debanding model of the aorta in mice.

First, we would like to congratulate the reviewer for the amazing paper that was central to this field and therefore a cornerstone to our research.

In the beginning, we used silk to perform the constriction due to its natural characteristics and considering that it slides less after tightening the knot. However, as silk is a multifilament suture, it imposes increased time and difficulty to loosen the knot during the debanding surgery. Nevertheless, we realized that its use is associated with a smaller percentage of suture internalization. The next obvious choice would be polypropylene, even if this material is more slippery. We overcame this problem by using a double surgeon's knot followed by a simple knot. Both knots were performed simultaneously around the 26-gauge needle. To be as fast as possible we used a long suture and held the 2nd knot with two hemostats allowing to tighten the 2nd knot quickly.

Concerning suture internalization in rats, we surpassed this issue by using a smaller polypropylene suture size for banding (6-0). Also, when this phenomenon was observed, aortic gradients decreased and, therefore, the animals had to be excluded. These small technical issues are widely protocol-and-operator-dependent, and these variations are not incompatible with good technical practices and reproductive results (Table 2).

It seems that the authors in the description of the surgery advocate using a left lateral thoracotomy for both banding and debanding. In our study, we advocated using a left lateral thoracotomy for the banding and a sternotomy for the debanding to reduce the rate of complications due to adhesions. In the discussion (lines 355-358), the use of a mini-

sternotomy is advocated. This should be pointed out also under the description of the surgery.

In the beginning of our surgical training, we used thoracotomy for the debanding surgery. However, later on, we found that mini left-side thoracotomy seemed to be preferable due to its less invasive and its shortest recovery time. Also, we observed that mini left-side thoracotomy improved the success of the open-chest hemodynamic performed two weeks later (Table 2).

The authors use Doppler aortic flow velocities above 2.5 m/s corresponding to a pressure gradient of 25 mmHg as cut-off to verify successful banding and debanding (line 212 and 277). We used 3 m/s corresponding to a pressure gradient of 36 mmHg as cut-off to verify successful banding and did not see any signs of increased velocities at the banding site following debanding in virtually any animal and no measurable gradient in any animal. However, we used silk suture for the banding and were careful to remove constricting fibrosis during debanding surgery to see a normalization of the aortic wall. In my opinion a narrow cut-off point of above 25 mmHg before debanding and below 25 mmHg after debanding seems inadequate. Following debanding the velocity at the constriction site should be similar to the velocity at the level of the aortic valve/root. The authors advocate heart rate above 400 beats per minute corresponding to light anesthesia and in my experience this would usually correspond to 1 m/s flow velocity at the level of the aortic valve/root. In figure 5A this velocity in sham operated animals is only 0.5 m/s. 2.5 m/s at the banding site and 0.5 m/s at the level of the aortic valve/root indicates in my opinion probably a significant stenosis and cardiodepression due to the depth of anesthesia.

We have to be honest and inform the reviewer that our lab echocardiographic equipment is not able to measure velocities above 2.5 m/s. Therefore, we recognise this is a study limitation. At the debanding surgery, we only removed the suture, not fibrosis, and the normalization of the aortic flow velocities was often partial but never reached the 2.0 m/s. Due to this equipment limitation, our flow velocities measurements were not quantitative. We only evaluate aortic flow (together with 2D color Doppler) to assess the constriction and compare it between groups. Therefore, the position and angle of the echo probe was not very accurately adjusted but just the enough to confirm the lower velocities in the sham groups images. The probe was not placed at the aortic root since the turbulent aortic flow in banding and thus the increases velocities occur at the point and immediately after the constriction. Before constriction, the velocities are lower than normal because as the blood has to go through a narrow space, it accumulates upstream. Your concern regarding the lower aortic velocities in sham are legitimate and a cardiodepression induced by over-anaesthesia could indeed reduce aortic velocities in parallel to decreased inotropy. However, chronotropism seems to be maintained as the heart rate in this image does not seem to be lower than normal.

Minor Concerns:

Line 35: The authors state that they have developed a banding-debanding model. As the model already is described previously I do not find the word "developed" appropriate. *We agree with the reviewer and toned down our words.*

Line 128: "Ascending aortic banding surgery (Rockman's technique)". Howard Rockman described in 1991 the model of transverse aortic constriction, not the ascending aorta.

The reviewer is correct. All the surgical procedure is similar, but the constriction is in a different aortic location. We added references reporting ascending aorta constriction.

Line 212: T*Preparation of the s*he phrase "by using both pulse wave Doppler" is not meaningful.

The text was changed accordingly.

1. Janssen SP, Gayan-Ramirez G, Van den Bergh A, Herijgers P, Maes K, Verbeken E and Decramer M. Interleukin-6 causes myocardial failure and skeletal muscle atrophy in rats. *Circulation*. 2005;111:996-1005.
2. Kim KH, Kim HK, Chan SY, Kim YJ and Sohn DW. Hemodynamic and Histopathologic Benefits of Early Treatment with Macitentan in a Rat Model of Pulmonary Arterial Hypertension. *Korean circulation journal*. 2018;48:839-853.